Science and Technology Indonesia
e-ISSN:2580-4391 *p*-ISSN:2580-4405
Vol. 7, No. 1, January 2022

Research Paper

Unique Adsorption Properties of Cationic Dyes Malachite Green and Rhodamine-B on Longan (*Dimocarpus longan*) Peel

Risfidian Mohadi[1,3]*, Normah[3], Erni Salasia Fitri[2], Neza Rahayu Palapa[2]

[1]*Graduate School of Mathematics and Natural Sciences, Faculty of Mathematics and Natural Sciences, Sriwijaya University, Palembang, 30662, Indonesia*
[2]*Research Center of Inorganic Materials and Coordination Complexes, Faculty of Mathematics and Natural Sciences, Sriwijaya University, Palembang, 30662, Indonesia*
[3]*Magister Programme Graduate School of Mathematics and Natural Sciences, Sriwijaya University, Palembang, 30662, Indonesia*
***Corresponding author**: risfidian.mohadi@unsri.ac.id

Abstract
This research converts agricultural waste Longan (*Dimocarpus longan*) Peel is used in the adsorption process to reduce cationic dyes rhodamine-B and malachite green contaminants from aqueous solution. Longan (*Dimocarpus longan*) Peel was characterized by FT-IR, analysis XRD, SEM, BET, and TG-DTA. The characterization results show that Longan (*Dimocarpus longan*) Peel contains cellulose compounds and has a specific surface area 17.175 m^2/g, with this Longan (*Dimocarpus longan*) Peel has the potential as a bio adsorbent. The adsorption capacity is proven by adsorption capacity (Q_m) shows that the bioadsorbent adsorption of malachite green has a large adsorption capacity of 182.64 mg/g, while the adsorption capacity of rhodamine-B (Q_m) reaches 52.557 mg/g and this bioadsorbent longan (*Dimocarpus longan*) peel is effective the adsorption was stable until the third cycle.

Keywords
Bioadsorbent, Longan, Malachite Green, Rhodamine-B, Adsorption

Received: 14 October 2021, Accepted: 24 January 2022
https://doi.org/10.26554/sti.2022.7.1.115-125

1. INTRODUCTION

Water is the most important resource and is needed by humans, living things, and plants. Water is essential for life on earth and accounts for up to 70.9% (Tariq et al., 2020). However, many industries are growing rapidly nowadays, so many industries directly dispose of their waste into the environment without treating it first (Karthikeyan and Meenakshi, 2020). Finally, it can pollute water which can affect human life, living things, and the environment. Globally, environmental pollution is an important problem, especially in developing countries. About 10,000 synthetic dyes are discharged into the environment directly (Fang et al., 2021). Among other waste pollutants, textile dye pollutants have become the main contaminants. This textile dye is very dangerous because it is carcinogenic (Ali et al., 2020), toxic (Ting et al., 2021), exhibits teratogenic effects, and can affect photosynthesis in water bodies. The dyes that are widely used in industry are malachite green and rhodamine B, which are cationic dyes that are very soluble in water so they are considered dangerous and cause cancer (Cheng et al., 2018), respiratory disease kidney failure, and are ecotoxicologically threatening the environment (Kumari et al., 2020). Malachite green is a commonly used dye and its molecular structure is shown in Figure 1a, while rhodium b its molecular structure is shown in Figure 1b.

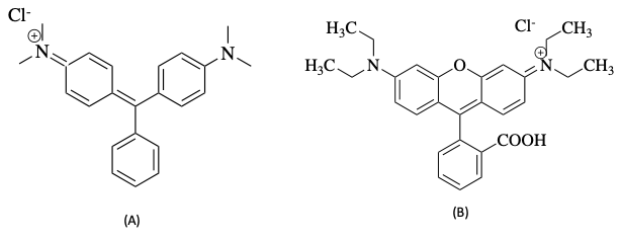

Figure 1. Chemical Structure of Malachite Green (a) and Rhodamine-B (b)

Therefore, the removal of dyes from textile waste is a major concern of researchers around the world. Conventional methods such as chemical coprecipitation (Mamat et al., 2018), flocculation, coagulation, precipitation, membrane filtration, degradation by microorganisms, and adsorption methods (Ahmed et al., 2020; Normah et al., 2021; Qu et al., 2019). Among all the methods, the adsorption process is found to be useful and common because it is cost-effective, easy to operate, and highly efficient (Fang et al., 2021). Recently, the application of bioadsorbents for pollutant adsorption has developed as an interesting research area. The high-performance adsorption

materials mainly include activated carbon, nano metal oxide, graphene (Alam and Al Riyami, 2018), zeolite, pulp, and bioadsorbent (Ma et al., 2021). Bioadsorbents have been widely used because of their environmentally friendly materials, low operating costs, thermal stability, higher cation exchange capacity, easy regeneration, and larger surface area. In addition, utilizing low-cost materials, namely agricultural waste. Agricultural waste bioadsorbents that are often used include sawdust, rice husks, walnut shells, longan peel, rambutan peel, duku peel, amarindus indica fruit shells (Vasu, 2007), langsat (*Lansium domesticum*) shell (Kurniawati et al., 2021), corn cob (Ismail et al., 2018), Napier grass stem (Tongpoothorn et al., 2019) and langsat shell (Kurniawaty, 2019), orange peel, banana peel (Yonika, 2021), and lemon peel. The dye waste as an adsorbent will interact and enter bound to the pores of the adsorbent so that the waste after the adsorption process will reduce pollutant levels.

Ismail et al. (2018) reported that corn cobs activated with sulfuric acid had an adsorption capacity of up to 98% for malachite green adsorption. Tariq et al. (2020) reported rhodamine-B can be degraded using the photo-Fenton process (homogeneous photocatalysis) was reached to be 86% at optimal pH=3 and degraded to 98%. Cellulose bioadsorbent made from Napier grass stalks to remove malachite green from this game. Napier grass stems showed that the maximum adsorption capacity reached 32.27 mg/g within 90 minutes. Based on the research of Kurniawati et al. (2021) the metals Cd(II) and Pb(II) which were adsorbed using longan seeds and peel produced optimal conditions used for Cd (pH 5) and Pb (pH 3). The results showed that the absorption of Pb metal ions for longan peel and longan seeds reached 42.14% and 57.07%, and Cd metal ions for seeds and longan shells reach 68.11% and 64.77%. The potential of langsat shell powder (*Lansium domesticum*) to adsorb rhodamine-B with an adsorption capacity of 12.3743 mg/g (Adella and Kurniawati , 2020).

Waste is longan peel can be used as an environmentally friendly adsorbent. Longan is a Sapindaceae plant shown in Figure 2, it has been commercially cultivated in many areas such as China, Taiwan, Vietnam, Thailand, especially Indonesia. This fruit has a sweet taste and has positive benefits for health. Longan peel contains active compounds such as phenolic acids, polysaccharides, and flavonoids so longan peel has the potential to be a low-cost heavy metal bioadsorbent (Rahmanian et al., 2018). The abundance of The active site of the main component of longan skin is what allows longan skin to have an excellent ability to remove pollutants from aqueous solutions (Wang et al., 2016b). Longan (*Dimocarpus longan*) peel contains gallic acid ($C_7H_6O_5$), flavone glycosides, and hydroxynamic with the main content of flavones in the form of quercetin and kaempferol (Albo et al., 2021). The compounds contained in it contain various functional groups that can interact directly with the adsorbate used, so longan peel is good to use as an adsorbent (Chen et al., 2017).

In this study, the peel of longan (*Dimocarpus longan*) was prepared into a bioadsorbent and used as an adsorbent of malachite green and rhodamine-B from aqueous solutions. Factors affecting the effectiveness of adsorption were studied through the selectivity of the dye mixture, the effect of pH, adsorption contact time, initial concentration, and adsorption temperature as well as the adsorbent regeneration process.

Figure 2. Indonesian Longan (*Dimocarpus longan*)

2. EXPERIMENTAL SECTION

2.1 Chemicals and Instrumentations

Chemicals such as hydrochloric acid, acetone, hydroxylamine chloride, ethanol, ethylene diamine tetraacetate (EDTA), sodium hydroxide, malachite green, rhodamine-B (Merck and Sigma Aldrich). Water was obtained from using Purite® ion exchange water purification process. The bioadsorbent of longan (*Dimocarpus longan*) was obtained from the local logan at Palembang, South Sumatera, Indonesia.

Characterization of bioadsorbent longan (*Dimocarpus longan*) was performed using FTIR Shimadzu Prestige-21 using KBr pellet and scanning sample at 400-4000 cm^{-1}. Surface area analysis was performed using the BET Nova 400e Omnisorp apparatus. The sample was evacuated under liquid nitrogen before analysis. The morphology of bioadsorbent was measured using (SEM) SU 8000 series following analysis of the composition of bioadsorbent using EDX. Analysis of thermal was conducted using Thermogravimetry-Differential Thermal Analysis (TG-DTA) Shimadzu DTG-60H. The structure of bioadsorbent was analyzed using XRD Rigaku-6000. The concentration of dyes was analyzed using a Biobase BK-1800 PC spectrophotometer. Malachite green and rhodamine-B were analyzed at 617 nm and 554 nm, respectively.

2.2 Preparation of Bioadsorbent and Characterization

Bioadsorbent of longan (*Dimocarpus longan*) was prepared prior used for bioadsorbent of malachite green and rhodamine-B. Longan (*Dimocarpus longan*) shell was washed with ethanol and water, respectively for several times and dried at 110°C for several days. Longan (*Dimocarpus longan*) shell was grounded by mortar until passed through a 100 mm sieve. Characterization of longan (*Dimocarpus longan*) shell was performed by FTIR spectroscopy, surface area measurement, thermal analysis, morphology and composition analysis by SEM-EDX, and structure analysis by XRD.

2.3 Adsorption Experiment

Several factors of adsorption were investigated such as the effect of pH, effect of adsorption time, effect of concentration of cationic dyes, and temperature. The desorption process and regeneration of bioadsorbent were also studied.

The effect of pH was studied through variation of pH of adsorption medium at 2-10 and the amount of adsorbed by analyzed. Adsorption time was studied by variation of adsorption time at 5-200 minutes with constant stirring on the batch adsorption system. Adsorption of malachite green and rhodamine-B using various initial concentrations and temperature was studied at 30, 40, 50, and 60°C with a concentration of dyes was 50-85 mg/L for malachite green and 5-12 mg/L for rhodamine-B.

Desorption of dyes on bioadsorbent was performed using various reagents such as water, hot water, EDTA, hydroxylamine chloride, ether, ethanol, acetone, hydrochloric acid, and sodium hydroxide. The highest desorption reagent will be used for the regeneration process. Regeneration was conducted 3 times after adsorption of dyes using the same sample from the fresh, first, and second adsorption process.

3. RESULTS AND DISCUSSION

The FT-IR spectrum of longan (*Dimocarpus longan*) is shown in Figure 3. It can be seen that logan (*Dimocarpus longan*) appears a significant and wide peak at the wavenumber of 3433 cm^{-1} which corresponds to the –OH stretching vibration. According to Shaikhiev et al. (2022); Nor et al. (2015) the wave number at 2931 cm^{-1} can be associated with C–H vibrations in both the $-CH_2$ and $-CH_3$ functional groups (Wang et al., 2016a; Zhang et al., 2016). The wavenumbers 2337 cm^{-1} characteristic peaks of C=C and 1627 cm^{-1} can be attributed to the vibrations of the C=O group of the aromatic ring. In addition, the wavenumber at 1230 cm^{-1} can be associated with C–C with C–O stretching, and 1056 cm^{-1} have a peak associated with the vibration of the C–O group. Vibrations that appear in the FT-IR spectrum of longan (*Dimocarpus longan*) indicate that logan i contains cellulose, hemicellulose, and lignin (Ikhtiari et al., 2015; Kaykhaii et al., 2018).

The bioadsorbent longan (*Dimocarpus longan*) was analyzed using the nitrogen adsorption-desorption analysis shown in Figure 4. Figure 4 shows that the isotherm pattern in Figure 4 shows that the material follows the type IV, isotherm model.

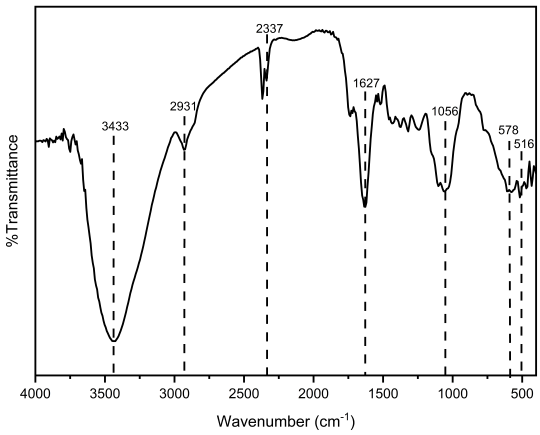

Figure 3. FTIR Spectrum of Logan (*Dimocarpus longan*)

Type IV isotherm indicates that the formation of multilayer and hysteresis phenomenon occurs (Brame and Griggs, 2016). Hysteresis is a material that has non-uniform pores so that adsorption-desorption does not overlap and there is a difference between nitrogen adsorption and desorption. According to Moller and Pich (2017), the type IV isotherm shows hysteresis with mesopore material with a size of 2-50 nm. Hysteresis on bioadsorbent longan (*Dimocarpus longan*) belongs to type H2. In type H2, this wide loop has a heterogeneous pore structure with sizes ranging from 2-6 nm and more than 10 nm in size. Thus, adsorption-desorption differences occur because they have heterogeneous sizes due to the blockage of smaller pores with a pore shape like a pile of paper with looser gaps (Grabi et al., 2021).

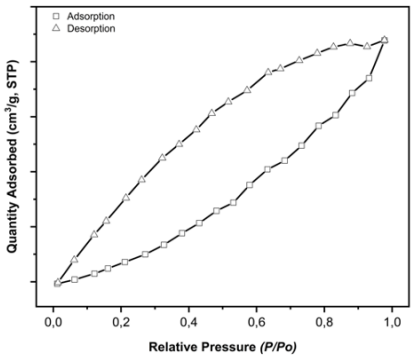

Figure 4. N_2 Isotherm Adsorption-Desorption of Longan (*Dimocarpus longan*)

The BET analysis data are presented in Table 1. Table 1 shows that the surface area of Bioadsorbent longan (*Dimocarpus longan*) is 17.175 m^2/g with a pore volume of 0.02 cm^3/g and a pore diameter of 12.33 nm. At lower temperatures, the bioadsorbent exhibits a relatively small surface area, due to insufficient carbonization. This indicates that the obtained carbon-

containing almost no finite pore framework. The temperature of the bioadsorbent preparation greatly affects the number of pores because the cracking process can control the number of pores due to the cracking of the carbon basalt structural sheet from the carbon particle basalt structural sheet (Kalak et al., 2021).

Table 1. BET Analysis of Logan (*Dimocarpus longan*)

Bioadsorbent	Surface area (m^2/g)	Pore volume (cm^3/g)	Pore diameter (nm)
Longan	17.175	0.02	12.33

Analysis of TG-DTA longan (*Dimocarpus longan*) from Figure 5. The differential thermal analyzer (DTA) method can be seen in black graphs to detect any thermal changes associated with exothermic or endothermic chemical events or reactions. This event can be seen in the form of a differential thermogram as maximum and minimum peaks. The maximum peak indicates an exothermic event where heat will be released by the sample. Figure 5 shows the results of the analysis of longan (*Dimocarpus longan*) with the appearance of an endothermic peak indicating a water loss of 100°C. The exothermic peak between 320°C and 500°C appears to be related to the decomposition of functional groups with lower stability of longan material (*Dimocarpus longan*) where the decomposition of cellulose and lignin occurs.

Table 2. Comparison of Surface Area Properties of Several Bioadsorbent

Bioadsorbent	Surface Area (m^2/g)	References
Aphanothece sp.	0.571	(Satya et al., 2020)
Aloe Vera powder	13.8	(Moosa et al., 2016)
Sugarcane Bagasse	0.991	(Priyanto et al., 2021)
Banana peel	0.32	(Kusrini et al. , 2019)
Pineapple peel	1.99	(Pathak et al., 2015)
Orange Peel	2.14	(Pathak et al., 2015)
Longan (*Dimocarpus longan*)	17.175	This Research

It can be seen that Table 2 shows that Longan (*Dimocarpus longan*) has a larger surface area compared to other bioadsorbents, this strongly supports the potential and ability of Longan (*Dimocarpus longan*) as an adsorbent to remove dyes and metals in waste.

Figure 6 shows the results of SEM analysis with the surface morphology of the longan peel (*Dimocarpus longan*) at a magnification of 100 m. In Figure 6(a) it can be seen that the cavities found on the surface of the bioadsorbent peel of the longan (*Dimocarpus longan*) fruit with morphology form aggregates of non-uniform size on the surface. The composition of the bioadsorbent longan (*Dimocarpus longan*) can be seen in Figure 6(b). Based on Figure 6(b) above, shows that the highest percentage of composition mass is carbon. According to Chang and Li (2019) longan (*Dimocarpus longan*) can bind to adsorbate due to the presence of active groups in the form of hydroxide

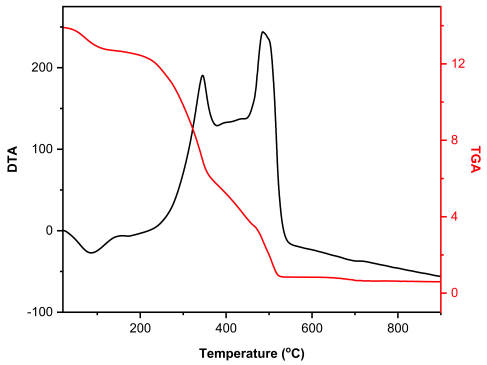

Figure 5. TG-DTA Profile of Longan (*Dimocarpus longan*)

(-OH), amine (-NH) aldehyde (-COH), and carboxyl (-COO) which can interact with the adsorbate and according to Lestari (2019) results from FTIR of longan (*Dimocarpus longan*) peel according to the composition of the SEM results.

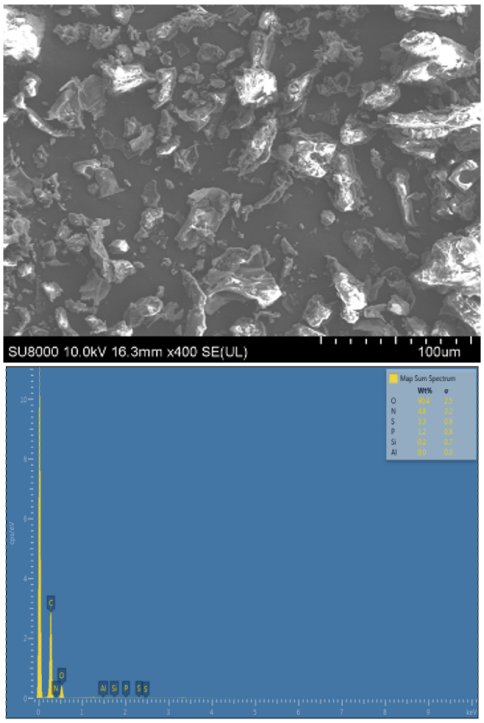

Figure 6. Surface Morphology and Composition of Longan (*Dimocarpus longan*)

Figure 7 shows the X-ray diffractogram pattern for the bioadsorbent longan (*Dimocarpus longan*). Figure 7 shows a wide peak with a diffraction angle of 23.05° with a diffraction plane (002) indicating that the longan bioadsorbent (*Dimocarpus longan*) has low crystallinity, indicating the characteristics of amorphous cellulose compounds due to the influence of lignin and hemicellulose (Oliveira et al., 2016). Characterization with X-Ray Diffraction (XRD) can be used as supporting data to determine the diffraction angle of the bioadsorbent from

longan (*Dimocarpus longan*).

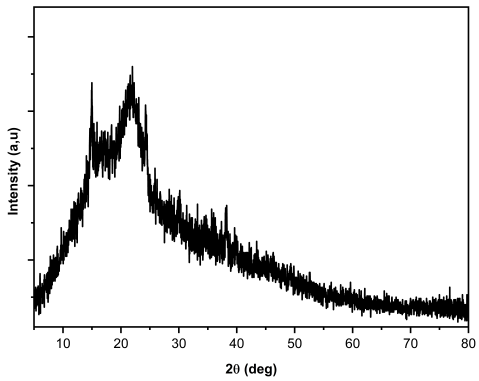

Figure 7. XRD Pattern of Logan (*Dimocarpus longan*)

The adsorption selectivity was carried out by mixing two dyes, namely malachite green (MG) and rhodamine-B (Rh-B), with a concentration of 8 mg/L and added bioadsorbent and the maximum wavelength of the mixture was measured using a UV-Vis spectrophotometer from 540 to 700. The results of these measurements are presented in Figure 8. The adsorption selectivity of the mixed dyes was analyzed from changes in the concentration of the adsorbed which were increasing during the adsorption process from 0, 15, 30, 60 to 90 minutes and carried out at variations of pH 4, 7, and 9. Figure 8 shows the results of adsorption selectivity at pH 4 on MG dye with an initial concentration of 8.31 mg/g rambutan peel became 4.11 mg/g, initial concentration of Rh-B dye 9.19 mg/g became 2.56 mg/g. The condition of pH 7 in the initial concentration of MG dye was 10.96 mg/g to 6.37 mg/g, the initial concentration of Rh-B dye was 10.42 mg/g to 3.21 mg/g. The condition of pH 9 on the initial concentration of MG dye was 9.16 mg/g to 3.37 mg/g, the initial concentration of Rh-B dye was 10.12 mg/g to 5.1 mg/g. A drastic decrease occurred at minute 120 with different pH conditions. It can be concluded that the selective dye for bioadsorbent is MG dye at alkaline pH (pH=9). After knowing the most selective dye, then proceed with the regeneration adsorption process isotherm adsorption and thermodynamic adsorption.

Measurement of the optimum pH for adsorption of malachite green dye to longan (*Dimocarpus longan*) bioadsorbent was carried out using variations of pH 2, 3, 4, 5, 6, 7, 8, 9, 10, and 11 with malachite green and rhodamine-B. The malachite green solution which has been adjusted to pH is then shaken for 120 minutes then its absorbance is measured using a UV-Vis spectrophotometer. The optimum pH of malachite green against longan (*Dimocarpus longan*) bioadsorbent can be seen in Figure 9(a) and the optimum pH for rhodamine-B is shown in Figure 9(b).

Based on Figure 9, obtained the optimum pH of malachite green dye is found at pH 6 and rhodamine-B is found at pH 4. pH has a direct influence on the mechanism of dye adsorption by the adsorbent. Figure 9(a) shows that there is an increase

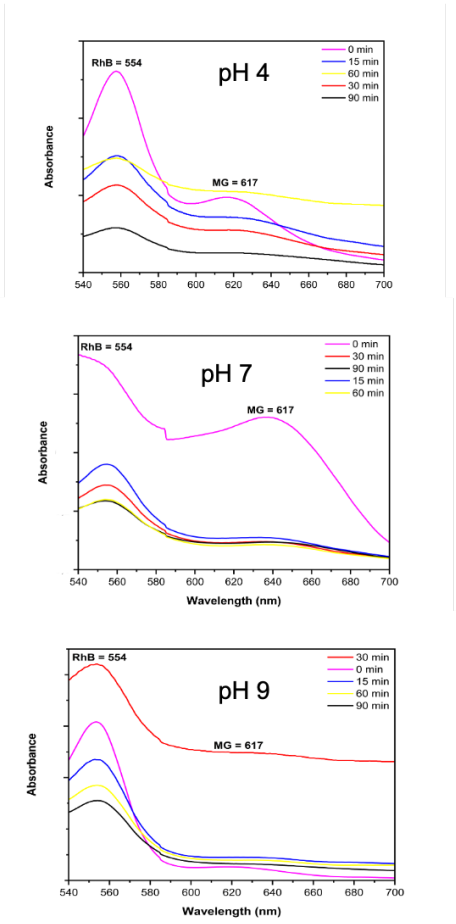

Figure 8. UV-Vis Spectrum of Dyes Mixtures After Adsorption at Several Times

in the adsorbed concentration with an increase in pH of 2-6 and the maximum is in the range of pH 6. However, there is a decrease in the adsorbed concentration when the pH reaches an alkaline pH. Moghadam et al. (2013) reported that when at acidic pH the surface of the adsorbent will experience protonation and act as a positive charge, but at alkaline pH, hydroxide ions (OH^-) will cause the exchange of Na^+ ions from the NaOH solution so that the active site on the adsorbent cannot interact with the adsorbent. dyes so that at alkaline pH the number of ions adsorbed decreases.

The effect of variations in the time of bioadsorbent longan (*Dimocarpus longan*) on malachite green and rhodamine-B can be seen in Figure 10. Figure 10 shows that for dyes the adsorption equilibrium time reaches 100 minutes. The data obtained were calculated using pseudo-first-order (PFO) and pseudo-second-order (PSO) kinetic model equations according to the literature (Juleanti et al., 2021). Adsorption kinetics data on variations in adsorption contact time are shown in Table 3.

Based on the kinetic data in Table 3 shows that the linear regression value (R^2) in the calculation of the pseudo-first-order kinetic model (PFO) tends to be closer to the value 1 compared

Table 3. Kinetic Model for Adsorption of Malachite Green and Rhodamine-B on Longan (*Dimocarpus longan*)

Dyes	Initial Concentration (mg/L)	Qe_{exp} (mg/g)	PFO			PSO		
			Qe_{Calc} (mg/g)	R2	k_1	Qe_{Calc} (mg/g)	R^2	k_2
MG	25	4.857	4.843	0.997	0.023	7.138	0.737	0.001
	50	6.536	9.480	0.785	0.035	0.514	0.866	3.415
	55	8.679	9.554	0.805	0.035	9.416	0.998	0.006
	65	11.893	13.210	0.775	11.489	0.059	0.235	4.509
Rh-B	4	1.178	1.049	0.931	0.035	1.284	0.997	0.051
	5	1.465	1.697	0.850	0.035	1.637	0.988	0.029
	6	1.835	9.016	0.928	28.949	32.581	0.743	9.458
	7	2.170	1.566	0.939	0.024	33.333	0.471	9.988

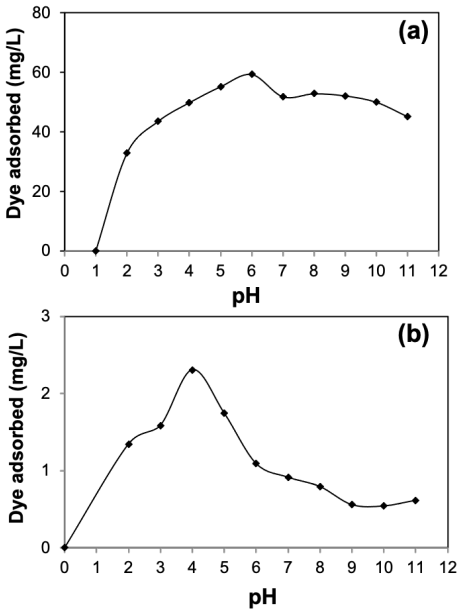

Figure 9. Effect of Various pH Adsorption of Malachite Green And Rhodamine-B on Longan (*Dimocarpus longan*)

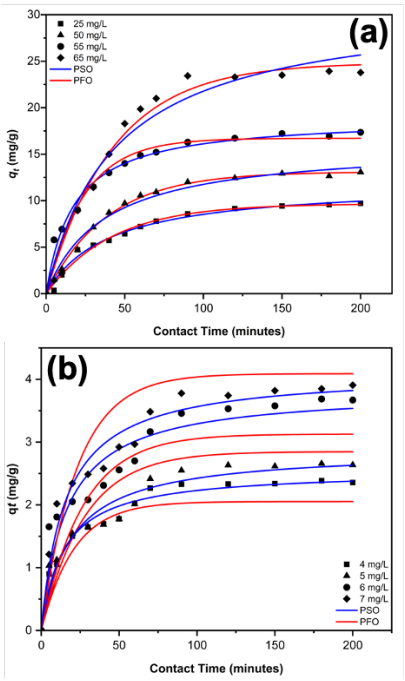

Figure 10. Effect of Adsorption Time Malachite Green (a); Rhodamin-B (b)

to the pseudo-first-order (PFO) kinetic model, it can be concluded that the adsorption of malachite green and rhodamine-B tends to follow the pseudo-first-order (PFO) equation for the bioadsorbent. Table 3 shows that the adsorbed concentration at equilibrium (experimental test) is directly proportional to the concentration used. According to Onder et al. (2020) the pseudo-first order (PFO) kinetic model indicates that adsorption tends to occur by physisorption with the adsorption equilibrium rate affecting only the adsorbent or adsorbate.

Figure 11 shows that as the adsorption temperature increases, it will cause an increase in the adsorbate adsorbed for each dye. The higher the concentration used, the more the adsorbed malachite green and rhodamine-B dyes will increase. Data on the effect of concentration and temperature on adsorption using bioadsorbents will then be used to determine the adsorption isotherm model using the Langmuir and Freundlich equation according to the literature (Wijaya et al., 2021). Langmuir and Freundlich's isotherm calculation of the data is shown in Table 4.

According to Zubair et al. (2018) Freundlich isotherm model assumes that the adsorbent surface is heterogeneous and supports multilayer adsorption and an adsorption process that occurs by physical (Wijaya et al., 2021), while the Langmuir isotherm assumes that adsorption occurs by the formation of a monolayer on the adsorbent surface that does not have interactions between adsorbate molecules (Mishra et al., 2020). The data in Table 4 shows that the Langmuir adsorption isotherm equation model has a linear regression

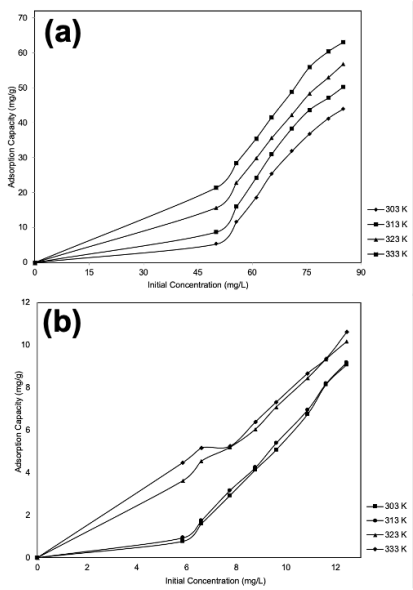

Figure 11. Thermodynamic Parameter Adsorption Malachite Green (a); Rhodamin-B (b) on Longan (*Dimocarpus longan*)

Table 4. Isotherm Parameter Adsorption of Malachite Green and Rhodamine-B on Longan (*Dimocarpus longan*)

Dyes	Temp. (K)	Model Isotherm Adsorption					
		Langmuir			Freundlich		
		Q_m	K_L	R^2	n	K_F	R^2
MG	30	1.829	0.027	0.964	0.114	1.428	0.984
	40	111.1	0.014	0.928	1.571	3.725	0.909
	50	158	0.02	0.93	1.749	5.336	0.949
	60	182.6	0.036	0.926	2.204	9.091	0.93
Rh-B	30	0.686	0.286	0.861	0.138	2295	0.859
	40	0.656	0.293	0.77	0.211	3254	0.813
	50	38.03	0.08	0.832	1.515	3.637	0.931
	60	52.56	0.137	0.863	1.139	4.017	0.89

value (R^2) which tends to be closer to the value 1 than the Freundlich adsorption isotherm equation for malachite green and rhodamine-B. Based on Table 4 the value of adsorption capacity (Q_m) shows that the bioadsorbent adsorption of malachite green has a large adsorption capacity of 182.64 mg/g, while rhodamine-B reaches 52.557 mg/g.

Furthermore, the thermodynamic parameters provide data on the (ΔG), (ΔH), and (ΔS) which are calculated according to the literature (Biesinger et al., 2011). The adsorption thermodynamic data are shown in Table 5.

Table 5 shows the results of the calculation of negative adsorption values for ΔG on each adsorbent. ΔG its value increased with increasing adsorption temperature reaching a ΔG value ranging from -0.190- to -1.923 kJ/mol. A negative value for ΔG indicates that the MB adsorption process takes place spontaneously (Lesbani et al., 2021) and the adsorption used in the adsorption process is better at high temperatures. The ΔH value showed a range of 27.495 kJ/mol (MG) and 23.066 kJ/mol (Rh-B) which was related to the tendency of malachite and rhodamine-B adsorption to occur by physical adsorption and a positive ΔH value indicated that MB adsorption was endothermic (Biesinger et al., 2011). The value of ΔS is positive, this is related to the irregularity of the particles during the adsorption process which increases due to the interaction between solid in the form of adsorbent-liquid in the form of malachite green and rhodamine-B adsorbate (Dang et al., 2020; Neolaka et al., 2020) .

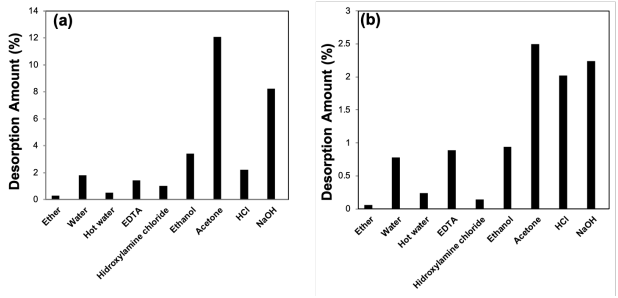

Figure 12. Desorption Process of Malachite Green (a) and rhodamine-B (b)

It can be seen in Figure 12 that the most suitable solvent for desorption of malachite green and rhodamine-B dyes using a bioadsorbent is acetone. Acetone solvent was able to release 12.08% malachite green and 2.5% rhodamine-B in the desorption process compared to other solvents. This shows that the interaction like dissolves like indicates and occurs between the dye adsorbate and the bioadsorbent from longan (*Dimocarpus longan*).

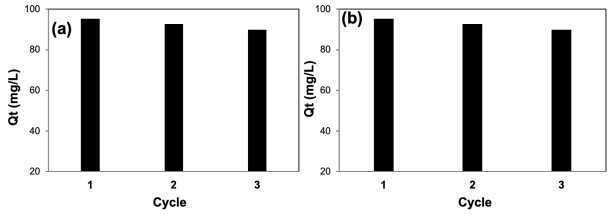

Figure 13. Cycling Bioadsorbent After Adsorption of Malachite Green (a) and Rhodamine-B (b)

Figure 13 shows the adsorption ability with repeated use. bioasorbent has adsorption capacity for the malachite green of 96.05% in the first cycle, its ability also decreased to 89.42% in the second cycle and the third cycle to 87.26%. The result of regeneration of rhodamine-B adsorption in the first cycle was 95.25%, the second cycle decreased to 10.13%. Zn/Al-Hc reached the first cycle of 94.13%, the second cycle of 90.54%, the third cycle of 89.73%, the fourth cycle of 84.21%, the fifth cycle of 80.12%, the sixth cycle of 78.33%, and the last is 78.11%. Bioadsorbent on longan (*Dimocarpus longan*) experienced an insignificant decrease. Based on these data, the bioadsorbent longan (*Dimocarpus longan*) has adsorption capacity with a regeneration cycle of up to a third.

Table 5. Thermodynamic Parameter Adsorption of Malachite Green and Rhodamine-B on Longan (*Dimocarpus longan*)

Dye	Concentration	T (K)	Q_e(mg/g)	ΔH (kJ/mol)	ΔS (J/mol.K)	ΔG (kJ/mol)
MG	85 mg/L	303	44.000	27.495	0.091	-0.190
		313	50.286			-0.768
		323	56.721			-1.345
		333	63.079			-1.923
Rh-B	12 mg/L	303	9.083	23.066	0.084	-0.090
		313	9.186			-1.181
		323	10.172			-2.273
		333	10.619			-3.365

The FT-IR spectrum in Figure 14 shows longan (*Dimocarpus longan*) before being adsorbed and after being adsorbed with the adsorbate. Figure 14 shows that there is a wavelength shift that is carried out by adsorption which will detect the functional group of the compound. the dye adsorption process is influenced by the number of functional groups, types of functional groups, interaction processes, adsorbent chemistry (Grabi et al., 2021). The results of the FT-IR spectrum can be seen in Figure 14 showing the appearance of a peak at the wavenumber of 2854 cm^{-1} because it has been in contact with the adsorbate. After treatment, strain vibrations of the S–O and S=O dye groups were observed at 1056 cm^{-1} and 1249 cm^{-1}. In addition, the bands at 1372 cm^{-1} and 1342 cm^{-1} came from the vibrations of amine groups from dye molecules. Thus, the FT-IR spectrum shows the displacement of certain functional groups and the appearance of functional groups from the dye on the surface of the bioadsorbent. The shift of peaks shows the interaction between rhodamine-B and malachite green dye ions with the surface of the bioadsorbent. The interaction can not only be seen in the shift of peaks but also seen from the intensity of each peak (Krishni et al., 2014).

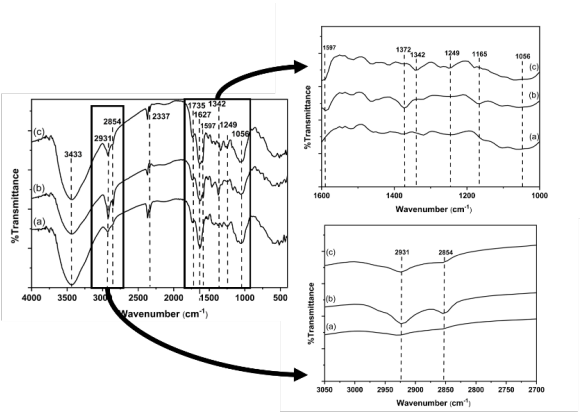

Figure 14. Spectrum FT-IR Before Adsorption (a), After Adsorption Malachite Green (b), After Adsorption Rhodamine-B (c) on Longan (*Dimocarpus longan*)

4. CONCLUSIONS

This study investigated waste longan (*Dimocarpus longan*) which was developed as a bioadsorbent to remove cationic dyes from aqueous solutions. adsorption capacity (Q_m) shows that the bioadsorbent adsorption of malachite green has a large adsorption capacity of 182.64 mg/g, while the adsorption capacity of rhodamine-B (Q_m) reaches 52.557 mg/g and this bioadsorbent longan (*Dimocarpus longan*) peel is effective the adsorption was stable until the third cycle.

5. ACKNOWLEDGEMENT

The author thanks the Research Center of Inorganic Materials and Complexes FMIPA Sriwijaya University for support of this research and also for analysis and instrumentation.

REFERENCES

Adella, F., and D. Kurniawati (2020). Adsorption of Rhodamine B from Aqueous Solution Using Langsat (*Lansium domesticum*) Shell Powder. In *International Conference on Biology, Sciences and Education (ICoBioSE 2019)*. Atlantis Press, 273–276

Ahmed, D. N., L. A. Naji, A. A. Faisal, N. Al-Ansari, and M. Naushad (2020). Waste Foundry Sand/MgFe-Layered Double Hydroxides Composite Material for Efficient Removal of Congo Red Dye from Aqueous Solution. *Scientific Reports*, **10**(1); 1–12

Alam, M. A. and K. Al Riyami (2018). Shear Strengthening of Reinforced Concrete Beam using Natural Fibre Reinforced Polymer Laminates. *Construction and Building Materials*, **162**; 683–696

Albo, J., M. I. Qadir, M. Samperi, J. A. Fernandes, I. de Pedro, and J. Dupont (2021). Use of an Optofluidic Microreactor and Cu Nanoparticles Synthesized in Ionic Liquid and Embedded in TiO_2 for an Efficient Photoreduction of CO_2 to Methanol. *Chemical Engineering Journal*, **404**; 126643

Ali, F., N. Ali, I. Bibi, A. Said, S. Nawaz, Z. Ali, S. M. Salman, H. M. Iqbal, and M. Bilal (2020). Adsorption Isotherm, Kinetics and Thermodynamic of Acid Blue and Basic Blue Dyes onto Activated Charcoal. *Case Studies in Chemical and Environmental Engineering*, **2**(9); 100040

Biesinger, M. C., B. P. Payne, A. P. Grosvenor, L. W. Lau, A. R. Gerson, and R. S. C. Smart (2011). Resolving Surface Chemical States in XPS Analysis of First Row Transition Metals, Oxides and Hydroxides: Cr, Mn, Fe, Co and Ni. *Applied Surface Science*, **257**(7); 2717–2730

Brame, J. A. and C. S. Griggs (2016). Surface Area Analysis using The Brunauer-Emmett-Teller (BET) Method: Scientific Operation Procedure Series: SOP-C. *U.S Army Engineer Research and Development Center*, **1**; 1–23.

Chang, C. C. and R. Li (2019). Agricultural Waste. *Water Environment Research*, **91**(10); 1150–1167

Chen, X., Q. Lin, R. He, X. Zhao, and G. Li (2017). Hydrochar Production from Watermelon Peel by Hydrothermal Carbonization. *Bioresource Technology*, **241**; 236–243

Cheng, Z.L., Y. X. Li, and Z. Liu (2018). Study on Adsorption of Rhodamine B onto Beta Zeolites by Tuning SiO_2/Al_2O_3 ratio. *Ecotoxicology and Environmental Safety*, **148**; 585–592

Dang, W., J. Zhang, H. Nie, F. Wang, X. Tang, N. Wu, Q. Chen, X. Wei, and R. Wang (2020). Isotherms, Thermodynamics and Kinetics of Methane-Shale Adsorption Pair Under Supercritical Condition: Implications for Understanding The Nature of Shale Gas Adsorption Process. *Chemical Engineering Journal*, **383**; 123191

Fan, X., Deng, L., Li, K., Lu, H., Wang, R., and Li, W (2021). Adsorption of Malachite Green in Aqueous Solution using Sugarcane Bagasse-Barium Carbonate Composite *Colloids and Interface Science Communications*, **44**; 100485

Grabi, H., F. Derridj, W. Lemlikchi, and E. Guénin (2021). Studies of The Potential of a Native Natural Biosorbent for The Elimination of An Anionic Textile Dye Cibacron Blue in Aqueous Solution. *Scientific Reports*, **11**(1); 1–13

Ikhtiari, R., H. Aziz, R. Zein, et al. (2015). The Removal of Cr(VI) with *Dimocarpus longan* as a Low Cost Biosorbent. *Journal of Chemical and Pharmaceutical Research*, **7**(9S); 81–88

Ismail, S. N. A. S., W. A. Rahman, N. A. A. Rahim, N. D. Masdar, and M. L. Kamal (2018). Adsorption of Malachite Green dye From Aqueous Solution using Corncob. In *AIP Conference Proceedings*, 2031; 020036

Juleanti, N., N. R. Palapa, T. Taher, N. Hidayati, B. I. Putri, and A. Lesbani (2021). The Capability of Biochar-Based CaAl and MgAl Composite Materials as Adsorbent for Removal Cr (VI) in Aqueous Solution. *Science and Technology Indonesia*, **6**(3); 196–203

Kalak, T., J. Walczak, and M. Ulewicz (2021). Adsorptive Recovery of Cd (II) Ions with The Use of Post-Production Waste Generated in the Brewing Industry. *Energies*, **14**(17); 5543

Karthikeyan, P. and S. Meenakshi (2020). Enhanced Removal of Phosphate and Nitrate Ions by a Novel ZnFe LDHs-Activated Carbon Composite. *Sustainable Materials and Technologies*, **25**; e00154

Kaykhaii, M., M. Sasani, and S. Marghzari (2018). Removal of Dyes from The Environment by Adsorption Process. *Chemical and Materials Engineering*, **6**(2); 31–35

Krishni, R., K. Foo, and B. Hameed (2014). Food Cannery Effluent, Pineapple Peel as an Efective Low-Cost Biosorbent for Removing Cationic Dye from Aqueous Solutions. *Desalination and Water Treatment*, **52**(31-33); 6096–6103

Kumari, S., A. A. Khan, A. Chowdhury, A. K. Bhakta, Z. Mekhalif, and S. Hussain (2020). Efficient and Highly Selective Adsorption of Cationic Dyes and Removal of Ciprofloxacin Antibiotic by Surface Modified Nickel Sulfide Nanomaterials: Kinetics, Isotherm and Adsorption Mechanism. *Colloids and Surfaces A: Physicochemical and Engineering Aspects*, **586**; 124264

Kurniawati, D., T. Sari, F. Adella, S. Sy, et al. (2021). Effect of Contact Time Adsorption of Rhodamine B, Methyl Orange and Methylene Blue Colours on Langsat Shell with Batch Methods. In *Journal of Physics: Conference Series*, 1788; 012008

Kurniawaty, D. (2019). Effect of Cadmium in Biosorption of Lead by Lengkeng Seed and Shell (*Euphoria logan lour*). *Journal of Chemical Natural Resources*, **1**(2); 23–29

Kusrini, E., Kinastiti, D. D., Wilson, L.D., Usman, A., Rahman, A (2019). Adsorption of Lanthanide Ions from an Aqueous Solution in Multicomponent Systems using Activated Carbon from Banana Peels (*Musa Paradisiaca L.*). *Journal of Chemical Natural Resources*, **19**; 1132–1139

Lesbani, A., N. R. Palapa, R. J. Sayeri, T. Taher, and N. Hidayati (2021). High Reusability of NiAl LDH/Biochar Composite in the Removal Methylene Blue from Aqueous Solution. *Indonesian Journal of Chemistry*, **21**(2); 421-434

Lestari, N. A. (2019). Reduction of CO_2 Emission by Integrated Biomass Gasification-Solid Oxide Fuel Cell Combined with Heat Recovery and in-situ CO_2 Utilization. *Evergreen*, **6**(3); 254–261

Ma, J., L. Hou, P. Li, S. Zhang, and X. Zheng (2021). Modified Fruit Pericarp as an Effective Biosorbent for Removing Azo Dye from Aqueous Solution: Study of Adsorption Properties and Mechanisms. *Environmental Engineering Research*, **27**(2); 200634

Mamat, M., M. A. A. Abdullah, M. A. Kadir, A. M. Jaafar, and E. Kusrini (2018). Preparation of Layered Double Hydroxides with Different Divalent Metals for The Adsorption of Methyl Orange Dye from Aqueous Solutions. *Chemical Engineering*, **9**(6); 1103–1111

Mishra, S., S. Sahoo, A. Debnath, K. Muthe, N. Das, and P. Parhi (2020). Cobalt Ferrite Nanoparticles Prepared by Microwave Hydrothermal Synthesis and Adsorption Efficiency for Organic Dyes: Isotherms, Thermodynamics and Kinetic Studies. *Advanced Powder Technology*, **31**(11); 4552–4562

Moghadam, M. R., N. Nasirizadeh, Z. Dashti, and E. Babanezhad (2013). Removal of Fe(II) from Aqueous Solution using Pomegranate Peel Carbon: Equilibrium and Kinetic Studies. *International Journal of Industrial Chemistry*, **4**(1); 1–6

Moller, M., and Pich, A (2017). Development of Modified Layered Silicates with Superior Adsorption Properties for Uptake of Pollutants from Air and Water. Development of

Modified Layered Silicates with Superior Adsorption Properties for Uptake of Pollutants from Air and Water Von. *Disertation*; University Zur Erlangung Des

Moosa, A., Ridha, A., Moosa, A.A., Ridha, A.M., Hussien, N.A (2016). Removal of Zinc Ions from Aqueous Solution by Bioadsorbents and CNTs Removal of Zinc Ions from Aqueous Solution by Bioadsorbents and CNTs. *International Journal of Industrial Chemistry*, **5**; 1–10

Neolaka, Y. A., Y. Lawa, J. N. Naat, A. A. Riwu, M. Iqbal, H. Darmokoesoemo, and H. S. Kusuma (2020). The Adsorption of Cr(VI) from Water Samples using Graphene Oxide-Magnetic (GO-Fe_3O_4) Synthesized from Natural Cellulose-Based Graphite (Kusambi Wood or Schleichera oleosa): Study of Kinetics, Isotherms and Thermodynamics. *Journal of Materials Research and Technology*, **9**(3); 6544–6556

Nor, N. M., T. Hadibarata, Z. Yusop, and Z. M. Lazim (2015). Removal of Brilliant Green and Procionred Dyes from Aqueous Solution by Adsorption using Selected Agricultural Wastes. *Jurnal Teknologi*, **74**(11); 117–122

Normah, N., N. Juleanti, P. M. S. B. N. Siregar, A. Wijaya, N. R. Palapa, T. Taher, and A. Lesbani (2021). Size Selectivity of Anionic and Cationic Dyes Using LDH Modified Adsorbent with Low-Cost Rambutan Peel to Hydrochar. *Bulletin of Chemical Reaction Engineering & Catalysis*, **16**(4); 869–880

Oliveira, E., J. Santos, A. Goncalves, S. Mattedi, and N. Jose (2016). Characterization of The Rambutan Peel Fiber (*Nephelium lappaceum*) as a Lignocellulosic Material for Technological Applications. *Chemical Engineering Transactions*, **50**; 391–396

Onder, A., P. Ilgin, H. Ozay, and O. Ozay (2020). Removal of Dye from Aqueous Medium with pH-Sensitive Poly [(2-(acryloyloxy) ethyl] Trimethylammonium Chloride-co-1-vinyl-2-pyrrolidone] Cationic Hydrogel. *Journal of Environmental Chemical Engineering*, **8**(5); 104436

Pathak, P.D., Mandavgane, S.A., Kulkarni, B.D. (2015). Fruit Peel Waste as a Novel Low-Cost Biodsorbent. *Reviews in Chemical Engineering*, **31**; 361-381

Priyanto, A., F, M., Muhdarina, M., A, A.(2021). Adsorption and Characterization of Activated Sugarcane Bagasse Using Natrium Hydroxide *Indonesian Journal Chemical Research*, **8**; 202-209

Qu, W., T. Yuan, G. Yin, S. Xu, Q. Zhang, and H. Su (2019). Effect of Properties of Activated Carbon on Malachite Green Adsorption. *Fuel*, **249**; 45–53

Rahmanian, O., M. Dinari, and M. K. Abdolmaleki (2018). Carbon Quantum Dots/Layered Double Hydroxide Hybrid for Fast and Efficient Decontamination of Cd (II): The Adsorption Kinetics and Isotherms. *Applied Surface Science*, **428**; 272–279

Satya, A., Harimawan, A., Haryani, G. S., Johir, M. A. H., Vigneswaran, S., Ngo, H. H., Setiadi, T (2020). Batch Study of Cadmium Biosorption by Carbon Dioxide Enriched *Aphanothece sp.* Dried Biomass. *Water*, **12**; 1–10

Shaikhiev, I. G., N. V. Kraysman, and S. V. Sverguzova (2022). Onion (*Allium Cepa*) Processing Waste as a Sorption Material for Removing Pollutants from Aqueous Media. *Biointerface Research in Applied Chemistry*, **12**(3); 3173–3185

Tariq, M., M. Muhammad, J. Khan, A. Raziq, M. K. Uddin, A. Niaz, S. S. Ahmed, and A. Rahim (2020). Removal of Rhodamine B dye from Aqueous Solutions using Photo-Fenton Processes and Novel Ni-Cu@ MWCNTs Photocatalyst. *Journal of Molecular Liquids*, **312**; 113399

Ting, A. S. Y., C. K. W. Cheng, and K. A. A. Santiago (2021). Decolourization of Malachite Green Dye by Endolichenic Fungi from The Lichen *Usnea sp.* : A Novel Study on Their Dye Removal Potential. *Journal of King Saud University Science*, **33**(7); 101579

Tongpoothorn, W., O. Somsimee, T. Somboon, and M. Sriuttha (2019). An Alternative and Cost-Effective Biosorbent Derived from Napier Grass Stem for Malachite Green Removal. *Journal of Materials and Environmental Sciences*, **10**(8); 685–695

Vasu, A. E. (2007). Biosorption of Rhodamine B and Malachite Green from Aqueous Aolutions by Tamarindus Indica Fruit Shells. *Current World Environment*, **2**(2); 127

Wang, L., A. Li, and Y. Chang (2016a). Hydrothermal Treatment Coupled with Mechanical Expression at Increased Temperature for Excess Sludge Dewatering: Heavy Metals, Volatile Organic Compounds and Combustion Characteristics of Hydrochar. *Chemical Engineering Journal*, **297**; 1–10

Wang, Y., L. Zhu, H. Jiang, F. Hu, and X. Shen (2016b). Application of Longan Shell as Non-Conventional Low-Cost Adsorbent for The Removal of Cationic Dye from Aqueous Solution. *Spectrochimica Acta Part A: Molecular and Biomolecular Spectroscopy*, **159**; 254–261

Wijaya, A., P. M. S. B. N. Siregar, A. Priambodo, N. R. Palapa, T. Taher, and A. Lesbani (2021). Innovative Modified of Cu-Al/C (C= Biochar, Graphite) Composites for Removal of Procion Red from Aqueous Solution. *Science and Technology Indonesia*, **6**(4); 228–234

Yonika, K. D. . K. M., S. (2021). Adsorption of Rhodamin-B Dyes using Active Carbon of Longan Shell (*Euphoria Longan lour*) with Batch Method. *International Journal of Scientific Research and Engineering Development*, **4**(5); 239–243

Zhang, J., M. Liu, T. Yang, K. Yang, and H. Wang (2016). A Novel Magnetic Biochar from Sewage Sludge: Synthesis and Its Application for The Removal of Malachite Green from Wastewater. *Water Science and Technology*, **74**(8); 1971–1979

Zubair, M., N. Jarrah, A. Khalid, M. S. Manzar, T. S. Kazeem, M. A. Al-Harthi (2018). Starch-NiFe-Layered Double Hydroxide Composites: Efficient Removal of Methyl Orange from Aqueous Phase. *Journal of Molecular Liquids*, **249**; 254–264

